Hybrid silica optical nanofibers for efficient Raman converters

Maha Bouhadida
Laboratoire Charles Fabry
Université Paris-Saclay, Institut d'Optique Graduate School, CNRS
Palaiseau, France
ORCID : 0000-0002-1676-4369

Aloïs Baudry
Laboratoire Charles Fabry
Université Paris-Saclay, Institut d'Optique Graduate School, CNRS
Palaiseau, France
alois.baudry@institutoptique.fr

Abderrahim Azzoune
Laboratoire Systèmes Lasers
Ecole Militaire Polytechnique
Algiers, Algeria
abderrahim.azzoune@emp.mdn.dz

Laurent Divay
Thales Research and Technology
Palaiseau, France
laurent.divay@thalesgroup.com

Etienne Eustache
Thales Research and Technology
Palaiseau, France
etienne.eustache@thalesgroup.com

Christian Larat
Thales Research and Technology
Palaiseau, France
christian.larat@thalesgroup.com

Jean-Charles Beugnot
Institut FEMTO-ST
line 3: *CNRS, Université Bourgogne, Franche-Comté*
Besançon, France
jean-charles.beugnot@femto-st.fr

Sylvie Lebrun
Laboratoire Charles Fabry
Université Paris-Saclay, Institut d'Optique Graduate School, CNRS
Palaiseau, France
sylvie.lebrun@institutoptique.fr

***Abstract*— Over the last twenty years, silica optical nanofibers have been widely exploited for a large range of potential applications in several areas of research such as atomic manipulation, plasmonic or sensing. Indeed, these devices present original properties of light propagation characterized by a high confinement of the optical mode in the uniform part and the presence of a strong evanescent field in the vicinity of the surface. This last property offers a new degree of freedom for the realization of nonlinear effects by changing the surrounding medium. We will firstly illustrate this option by generating Stimulated Raman Scattering with very high conversion efficiencies using nanofibers immersed in different liquids. Secondly, we will investigate the functionalization of nanofibers by coating them with thin layers of nonlinear materials. These studies open the way to the realization of low-cost and low-loss in-line devices based on hybrid silica optical nanofibers.**

Keywords—Optical Nanofiber, Stimulated Raman Scattering, coating, TiO₂, PMMA

I. INTRODUCTION

Optical nanofiber (ONF), i.e., the homogeneous section of a stretched and tapered silica optical fiber (sub-micrometer or micrometer diameter on length of up to more than 10 cm) between two tapered transitions, has been widely used in science and engineering applications since more than thirty years as an elementary optical device easily integrated by its nature in an all-fibered network [1]. Due to these intrinsic properties, ONF-based technologies have addressed a large versatility of domains from fundamental to applications such as quantum information devices (e.g. trapped atoms for quantum light-matter interfaces, photon-pair generation) [2,3], remote sensor devices [4], nonlinear optics (e.g. supercontinuum generation) [5] for the most active ones. The expanding use of ONF is due to its physical properties. The optical modes guided by the ONF have large intensities due to their strong transverse confinement, present very low losses (below 0.005 dB/cm, far beyond other micro/nano waveguides) and exhibit an evanescent part outside the ONF and therefore in interaction with the external medium. This latter property provides a new degree of freedom for achieving nonlinear effects by modifying the surrounding medium, a strategy that has been scarcely explored so far [6,7]. We will firstly illustrate this option by generating Stimulated Raman Scattering (SRS) in the visible range with very high conversion efficiencies using ONF immersed in different liquids. Secondly we will investigate the functionalization of ONF by coating them with thin layers of nonlinear materials to realize all-solid Raman converters in the telecommunication window. These studies open the way to the realization of low-cost and low-loss in-line devices based on hybrid silica ONF.

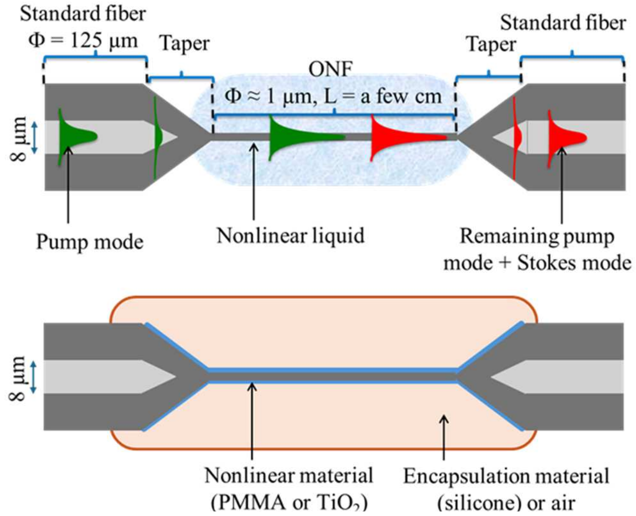

Figure 1. Top : geometry of the device and principle of Raman conversion based on the interaction of the pump mode evanescent field with the nonlinear liquid medium. Bottom : principle of the all-solid state Raman converter based on an ONF coated with thin layers of a nonlinear material. The device can be encapsulated for mechanical protection.

II. GENERAL DESIGN OF THE HYBRID ONF FOR THE REALIZATION OF RAMAN CONVERTERS

The hybrid ONF is either a two layer waveguide when immersed in a liquid (see Figure 1, top) or a three-layer waveguide when coated (see Figure 1, bottom). In the first case, the waveguide is constituted by the ONF and the immersing liquid which is considered as a medium of infinite

979-8-3315-9777-1/25/$31.00 ©2025 IEEE

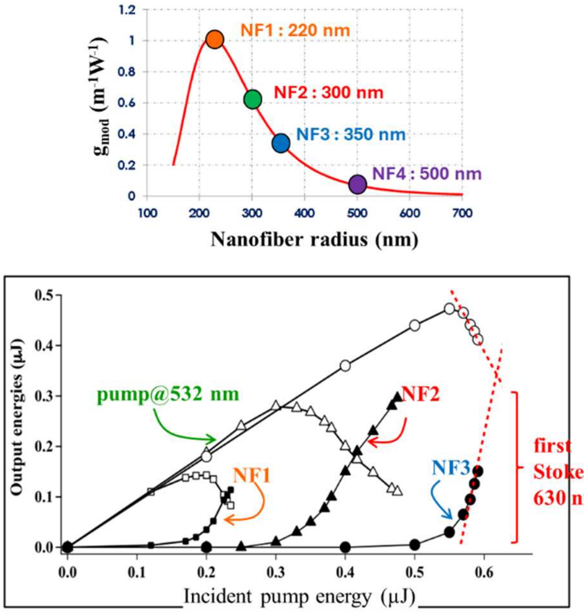

Figure 2. Top : Raman modal gain versus the ONF radius in ethanol. The tested radii are indicated. Bottom : Output energies at 532 nm and 630 nm versus the incident pump power for NF1, NF2 and NF3. For NF4, we observed the apparition of the first Stokes order of ethanol, even for the very low gain.

extension. In the second case, the waveguide is constituted by the ONF, the nonlinear material used for coating and the surrounding material that can be air or an encapsulation material. In the simulations we have performed, the thickness of the material used for encapsulation is considered as infinite. The length of the silica ONF is L and its radius is r_{NF}. To calculate the effective indexes of the modes at pump and Stokes wavelengths as well as the electric and magnetic fields, we have used a two layer vectorial model for the liquids or a three layer model in the scalar approximation for the coatings [8].

The key-parameter for the design of our devices is the Raman modal gain g_{Rmod} (in $m^{-1}W^{-1}$). The modal Raman gain is expressed following the analysis conducted in [9] by :

$$g_{Rmod} = \frac{\varepsilon_0^2 c^2 \int_{active\ area} g_{bulk} n_g^2 \left|e_p . e_s\right|^2 dA}{\left(\int_{total\ area} (e_p \times h_p) . z dA\right)\left(\int_{total\ area} (e_s \times h_s) . z dA\right)}$$

ε_0 is the dielectric permittivity of vacuum, c is the celerity of light in vacuum, dA is a unitary surface element and z is the direction of propagation. This gain is depending on the parameters of the nonlinear material which are its Raman gain coefficient g_{bulk} (in mW^{-1}) and its refractive index n_g; e and h represent, respectively, the electric and the magnetic fields; p and s stand for, respectively, pump and Stokes. We consider that the pump and the Stokes modes propagate on the fundamental mode which presents a revolution symmetry. By essence g_{Rmod} strongly depends on r_{NF} (see Figure 2, top).

The following approach was adopted: we firstly studied Raman converters in ethanol, a nontoxic and easy-to-manipulate liquid. We sized the device, i.e. its radius and its length, based on g_{Rmod}, to get Raman threshold before the laser-induced damage threshold (~1 kW). For the maximum length of 8 cm we can reach with our pulling rig, the radius should be in the range of 200 nm to 350 nm. We performed experimental demonstrations at 532 nm in the sub-nanoseconde regime (see paragraph IV). Then, we numerically investigated all-solid state Raman converters for an emission in the telecommunication range (see paragraph V). As we were able to observe SRS in liquids with peak pump powers of a few hundreds of W and moderate modal Raman gains that can be down to 0.2 $m^{-1}W^{-1}$, we targeted a modal Raman gain of 0.2 $m^{-1}W^{-1}$. A lower modal Raman gain can be compensated by a longer ONF or an increase of the input pump power. At last, we present preliminary results on the coating of ONF by two nonlinear materials, TiO_2 and PMMA.

III. STIMULATED RAMAN SCATTERING (SRS) IN THE EVANESCENT FIELD OF ONF IMMERSED IN LIQUIDS

In these studies, the ONF serves as the core of the optical waveguide and the cladding is the nonlinear medium constituted by the immersing liquid. The pump photons in the evanescent field scatter by SRS on the molecules of the liquid. Then the generated Stokes photons couple to a propagating mode of the ONF and are collected at the output of the end fiber (see Figure 1, top).

We have built an ONF pulling rig described in [6]. A butane flame softens the fiber central part while two computer-controlled translation stages elongate it following the classical "pull and brush" technique to create the ONF and its tapers. Our rig enables to produce routinely light transmission around 70% to 90% over the full device, i.e. the ONF part and its two tapers. The rig is placed in a class 5 clean-room to avoid the contamination by dusts. Once drawn, the ONF is transported in a tank in the laboratory and the tank is filled with the liquid. The pump source is a frequency-doubled Nd:YAG laser emitting beam at 532 nm with a pulse duration of 900 ps (FWHM), a frequency repetition rate of 4.7 kHz and a maximum available peak pump power of 7 kW. The pump beam is injected with a microscope objective in the untapered input end of the device and the output beams are collected on the other side and sent to an optical spectral analyzer.

As shown in Figure 2, bottom, conversion efficiencies from the pump source emitting at 532 nm to the first Stokes order of ethanol at 630 nm as high as 60% were obtained for an ONF radius of 300 nm [6]. Other ONF radii were tested (see Figure 2, top). We observed the apparition of the first Stokes order of ethanol even for a radius as high as 500 nm, corresponding to a very low gain of 0.07 $m^{-1}W^{-1}$. For a given pump wavelength, changing the immersing liquid enables to change the Stokes wavelength. We have tested other liquids such as isopropanol and toluene. The generated first Stokes order wavelengths were respectively 582 nm and 562 nm (for toluene we also observed the second Stokes order at 595 nm).

IV. DESIGN OF NEW ALL-SOLID RAMAN WAVELENGTH CONVERTERS BASED ON COATED ONF

Due to the absorption of liquids in the near infrared range, the above-described converters are optimized for visible wavelengths. Despite the depicted attractive features, the performances were limited by the optical breakdown of the ONF induced by the pump laser [10]. The absorption of the laser by surface defaults can lead to an increase of the temperature of the ONF and in its vicinity generating bubbles in the liquid that can degrade the optical transmission and even break the ONF.

In this part, we investigate new possibilities offered by silica ONF coated with thin films of nonlinear materials [11].

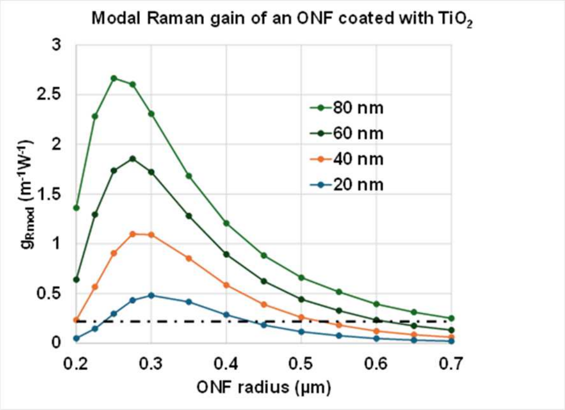

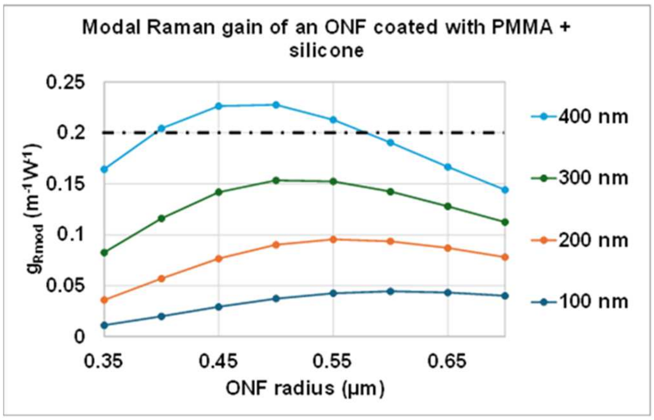

Figure 3. Modal Raman gain versus the ONF radius for a coating with TiO_2 (top) and for a coating with PMMA (bottom).

The aim is to build all-solid Raman wavelength converters in the pulsed regime based on these coated ONF. The light propagation is ensured by the ONF and the nonlinear photons produced in the coating layer couple to a propagating mode of the coated ONF. This mode is then collected at the output end fiber. Another advantage of coating ONF is to protect them from dust and pollutants that can affect their optical transmission.

The selected materials for the coatings are Titanium dioxyde (TiO_2) and Polymethyl methacrylate (PMMA). These materials are both transparent in the visible, near visible range and in the telecommunication window. TiO_2 is a highly nonlinear material and has been used for the realization of integrated waveguides under its crystalline phase [12]. The pump wavelength is 1.5 µm. As the Raman shift of TiO_2 is small (140 cm^{-1}), the first Stokes order wavelength is close, at 1.54 µm. PMMA is also an interesting material for nonlinear optics [13]. As an example PMMA optical fibers have been studied for Raman amplifier. The pump wavelength is 1.06 µm. The Raman shift of PMMA being 2957 cm^{-1}, the first Stokes order wavelength is at 1.53 µm.

For both materials, an original process for the coating of ONF with thin layers of controlled thicknesses has been developed and have been published in [14]. In this work, the targeted Stokes wavelengths are in the telecommunication window but they can be extended to other wavelength ranges where the materials are transparent.

A. Numerical studies

On Figure 3, we present the modal Raman gains versus the ONF radius in function of the thickness of the TiO_2 layer (top) and of the thickness of the PMMA layer (bottom). We can see that the targeted value of 0.2 $m^{-1}W^{-1}$ can be reached in both case, for realistic thicknesses of the deposited materials [14].

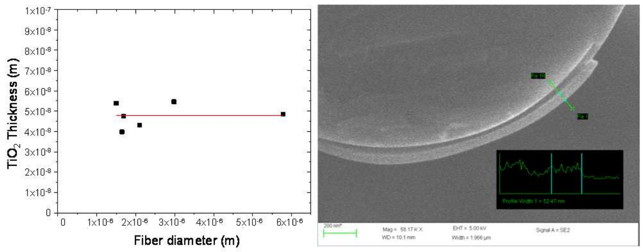

Figure 4. Left : Thickness of the deposited layer of TiO_2 versus the diameter of the ONF. Right : example of a SEM image of the cleaved fiber's cross section of an ONF coated with TiO_2.

B. TiO_2 coating

In the following, we present preliminary results obtained by coating ONF with TiO_2. A technique that is particularly well suited to metal oxide depositions is Atomic Layer Deposition (ALD). This technique is used in a primary vacuum chamber. A thin layer is progressively built on all the surfaces of the chamber and of the sample exposed to successive metal precursor vapor and oxidizing gas. Its thickness can be very precisely controlled. ALD is particularly adapted to the case of ONF since the deposition is non directional and a homogeneous thin layer can be deposited on the whole surface of this cylindrical component. The target thickness is 50 nm. On Figure 4, ONF with diameters varying between 1.3 µm and 6 µm have been coated, cleaved and the cross-sections have been observed by Scanning Electron Microscopy (SEM). We measured an average thickness of the deposited layer of 48 nm, very close to the target thickness and probably within the accuracy of the measuring procedure.

To measure the losses induced by the TiO_2 deposition, we have drawn an ONF with a diameter of 1 µm and a length of 2 cm. Then we have fusion-spliced its two untapered ends to two fibre pigtails. A laser beam at 1.5 µm has been injected in the component. The losses of the bare ONF with the two pigtails were 2 dB. After having coated the ONF with TiO_2 the losses increased to 2.5 dB, leading to additional losses of no more than 0.5 dB.

C. PMMA coating

Here, the coating process requires the use of liquid PMMA solution. Acetophenone is selected as solvent for its low toxicity and low vapor pressure for ease of handling and to avoid solvent evaporation during coating. The concentration of PMMA in the liquid solution is 264 g/L. The technique we have developed has been adapted from the classical dip-coating technique and is inspired by [15]. A drop of the solution is placed in a U-shape profile which is translated gently at a constant speed along the fiber in the horizontal direction, making the deposition. The fiber is then heated under reduced pressure in a vacuum oven to evaporate the solvent. By using this technique, the success rate of deposition without breaking the ONF is close to 100%. The thickness of the deposited layer depends on the radius of the ONF and is only around 10 nm. To get greater thicknesses, this process was used for a multiple deposition of PMMA. In Figure 5, six successive depositions were made with a vacuum drying step between each deposition. At the end of the process, the fiber was prepared for SEM observation. The successive coating process allows large thicknesses to be reached. For example,

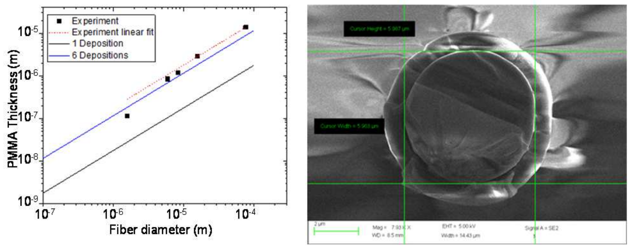

Figure 5. Left: thickness of the deposited layer of PMMA versus the diameter of the fiber. Square: experimental data. Comparison with the prediction of the model with one layer and 6 successive layers. Right: SEM image of an ONF coated with 6 layers of PMMA.

a thickness of 100 nm can be obtained on an ONF having a diameter of 1.5 µm (versus 10 nm with a single deposition pass).

We have also applied this technique successfully to the deposition of thin layers of PMMA doped with a nonlinear dye (Disperse Red 1). Other polymers can also be investigated for developing novel applications [16].

D. Encapsulation in silicone

In addition, we have studied the feasibility of encapsulating an ONF coated with PMMA in a low index medium. The challenge is to perform the encapsulation by preserving the PMMA layer and a good optical transmission. We have chosen silicone RTV elastomer as the encapsulation material since silicone resin has the advantage of being bulk polymerized for millimeter scale deposition thicknesses and is not a solvent of PMMA. We measured a refractive index after polymerization of 1.39, well below the refractive index of silica (1.45). This encapsulation would enable to enhance the mechanical resistance of the ONF by keeping the guidance at the same time. In this process the ONF is immersed in the silicone precursor. The liquid is then outgassed under vacuum and cured at ambient temperature for 48 hours. For this demonstration of principle, we pulled two fibers with a diameter of 10 µm. The fibers were fusion-spliced on both ends to two pigtails and their optical transmission of the components monitored with a tunable laser diode. The first fiber was encapsulated in silicone without PMMA coating. The average optical transmission from 1456 to 1548 nm increased from 48% in air to 57% in silicone, firstly validating the possibility to encapsulate tapered fibers in silicone without breaking them and secondly showing that this process does not induce important losses (the transmission even increased, due to the refractive index of silicone higher than the one of air). The second fiber was coated with PMMA and then encapsulated in silicone. After the two processes we measured an optical transmission of the fiber of 38%, which remains a high value. Even if further experiments and measurements need to be performed to optimize the coatings, this promising result validates the feasibility of this two-step treatment.

V. CONCLUSION AND PERSPECTIVES

We have presented two kinds of new all-fibered Raman converters based on the interaction of the evanescent field of propagating mode of silica ONF with the surrounding medium Firstly we immersed ONF in ethanol and demonstrated conversion efficiency from the pump source at 532 nm to the first Stokes order of the liquid at 630 nm as high as 60%. Several radii and liquids were tested, enlarging the possibilities of these ONF based devices. Secondly we have investigated the realization of all-solid Raman converters in the telecommunication range by coating ONF with nonlinear materials such as TiO_2 or PMMA. Simulations have shown that Raman threshold could be reached with experimentally achievable thicknesses of both materials. We have also presented preliminary experimental results on the coating of ONF with thin layers of both materials. Two different processes were developed: ALD for TiO_2 and multiple horizontal dip-coating for PMMA. Targeted thicknesses of respectively 50 nm for TiO_2 and 100 nm for PMMA were achieved. The losses obtained with TiO_2 are only 0.25 dB/cm. The use of PMMA as a coating is promising and warrants further refinement. More generally, these studies open the way to new applications in the field of nonlinear optics and lasers. For example, one can imagine tailoring the chromatic dispersion for the control of phase matching conditions or using other nonlinear materials such as doped polymers.

REFERENCES

[1] L. M. Tong, R. Gattass, J. Ashcom, S. He, J. Lou, M. Shen, I. Maxwell and E. Mazur, “Subwavelength-diameter silica wires for low-loss optical wave guiding”, Nature 426, 816-819 (2003).

[2] N. Corzo J. Raskop, A. Chandra, A. Sheremet, B. Gouraud and J. Laurat., Nature 566, 359 (2019).

[3] P. Delaye, T. Liu, E. Mer, M. Bouhadida, and S. Lebrun, “Continuous-wave generation of photon pairs in silica nanofibers using single-longitudinal- and multilongitudinal-mode pumps”, Phys. Rev. A, vol. 104, pp. 063715 (2021).

[4] L. Zhang, Y. Tang and L. Tong, “Micro-/Nanofiber Optics: Merging Photonics and Material Science on Nanoscale for Advanced Sensing Technology”, iScience 23(1), 100810 (2020).

[5] Y. Haddad, J. Chrétien, J.-C. Beugnot, A. Godet, K. Phan-Huy, S. Margueron, and G. Fanjoux, “Microscopic imaging along tapered optical fibers by right-angle Rayleigh light scattering in linear and nonlinear regime”, Optics Express, 29(24), 39159-39172 (2021).

[6] M. Bouhadida, J. C. Beugnot, P. Delaye, K. Phan Huy and S. Lebrun, "Highly efficient and reproducible evanescent Raman converters based on a silica nanofiber immersed in a liquid", Applied Physics B, Volume 125, Issue 12, pp.1-7 (2019).

[7] G. Fanjoux, J. Chrétien, A. Godet, K. Phan-Huy, J.-C. Beugnot, and T. Sylvestre, "Demonstration of the evanescent Kerr effect in optical nanofibers", Opt. Express 27, 29460-29470 (2019).

[8] A.W. Snyder and J. Love, (2012). Optical Waveguide Theory (Springer Science & Business Media).

[9] M.D. Turner, T. Monro and S. Afshar, “A full vectorial model for pulse propagation in emerging waveguides with subwavelength structures part II: Stimulated Raman Scattering”, Opt. Express 17(14), 11565–11581 (2009).

[10] M. Bouhadida, P. -E. Verdier and S. Lebrun, "Laser-Induced Damage in Silica Nanofibers in Air and Immersed in Different Liquids in the Nanosecond Regime", IEEE Photonics Technology Letters, vol. 33, no. 17, pp. 967-970 (2021).

[11] S. Lebrun., M. Bouhadida, T. Dampt, M. Fauvel, C. Larat, A. Azzoune, J.-C. Beugnot and L. Divay, “Design of composite optical nanofibers for new all-solid-state Raman wavelength converters”, J. Eur. Opt. Society-Rapid Publ. 20, 2 (2024).

[12] C. Evans, K. Shtyrkova, J. Bradley, O. Reshef, E. Ipen, and E. Mazur, “Spectral broadening in anatase titanium dioxide waveguides at telecommunication and near-visible wavelengths », Optics Express, 21 (15) 18582 (2013).

[13] K.J. Thomas, M. Sheeba, V. Nampoori, C. Vallabhan and R. Radhakrishnan, “Raman spectra of polymethylmethacrylate optical fibres excited by a 532 nm diode pumped solid state laser”, J. Opt. A : Pure Appl. Opt. 10 (2008) 055303 (5pp).

[14] L. Divay, E. Eustache, M. Bouhadida, C. Larat, A. Azzoune, J.-C. Beugnot, S. Lebrun, “Thin Layer Deposition of TiO2 and PMMA on Optical Micro or Nano Fibers for Nonlinear Optics”, J. Eur. Opt. Society-Rapid Publ., 21, 15 (2025).

[15] A. M. Velázquez-Benítez, M. Reyes-Medrano, J. R. Vélez-Cordero, and J. Hernández-Cordero, “Controlled Deposition of Polymer Coatings on Cylindrical Photonic Devices”, Journal of Lightwave Technology, vol. 33, Issue 1, pp. 176-182 (2015).

[16] F. Cherioux, P. Audebert, H. Maillotte, L. Grossard, F. E. Hernandez, and A. Lacourt, “ New Third-Order Nonlinear Polymers Functionalized with Disperse Red and Disperse Orange Chromophores with Increased Stability”, Chem. Mater. 1997, 9, 2921-2927.